








Multiangle, Frequency, and Polarization Radar Measurement of Ice Sheets

Jie-Bang Yan , *Member, IEEE*, Linfeng Li , Joshua A. Nunn , Dorte Dahl-Jensen, Charles O'Neill, Ryan A. Taylor , Christopher D. Simpson, Shashank Wattal , Daniel Steinhage, Prasad Gogineni, *Life Fellow, IEEE*, Heinrich Miller , and Olaf Eisen 

Abstract—Radio echo sounding of polar ice sheets provides important information on the ice bed topography and internal layers. These data have been used by scientists to create 3-D maps of polar ice sheets for climate modeling as well as to reconstruct the climate history that dates back to hundreds of thousands of years. In this article, we present the design and development of three surface-based multichannel radars in the VHF and UHF bands. We provide results from radar data multifrequency and polarization radar data collected over the Greenland ice sheet. All the three radars shared the same digital waveform generator and digitizer, and were installed in and operated on a tracked vehicle. The radars are operated with three different antenna arrays designed for operation over 170–230, 180–340, and 600–900 MHz. The results we obtained sounded more than 2.7 km thick ice with radars operating at frequencies as high as 850 MHz with more than 40 dB signal-to-noise ratio.

Index Terms—Greenland, ice, radar, radio echo sounding.

I. INTRODUCTION

UNDERSTANDING the ice sheets' response to warming atmosphere and ocean water and developing ice models to obtain more accurate estimates of sea-level change is critical to developing coastal protections. Greenland Ice Sheet (GrIS) and Antarctica Ice Sheet (AIS) are the two largest potential contributors to sea level rise. Measurements over the past decade

have shown that the GrIS has been losing mass at a much faster rate than model predictions [1]–[3]. Such discrepancy can largely be attributed to the lack of knowledge on the ice basal boundary conditions [4]. While airborne radar soundings of ice since the early 1970s have provided basal topography data to improve ice-sheet models, the basal conditions and the internal structure of ice sheets are still poorly represented. The presence of a thin film (1–10 mm) of subglacial meltwater could result in significant difference in the stress resisting ice flow [5]–[7]. The impact of ice sheets' microstructures and macrostructures on the ice flow along fast-flowing ice streams remains a topic of many investigations. Fine-resolution bed topography data together with detailed information on basal conditions and ice internal structure are necessary to constrain and improve existing ice models to predict the future evolution of ice sheets.

As a part of the East Greenland Ice-coring Project (EGRIP) [8] led by the University of Copenhagen, and ongoing research at the University of Alabama Remote Sensing Center, we developed three surface-based multichannel radar systems. These radars operate over three sub-bands (170–230, 180–340, and 600–900 MHz) to assist the study of ice streams and their dynamics, as well as their contributions to ice discharge and future sea-level change. As compared to airborne ice sounding radars, surface-based radars travel at much lower speed, thereby allowing an order of magnitude longer signal integration time to increase the signal-to-noise ratio (SNR) of returns from ice internal layers and ice-bedrock interface. Together with multi-angle and polarization measurement capabilities, these radars can image fine details of ice stratigraphy from the surface to bed. Together with repeated passes over a small target area, very detailed echograms of ice sheets can be produced. The proposed surface-based radar systems are designed to accomplish the following:

- 1) sound more than 3-km thick ice with two-way ice loss as high as 30 dB/km;
- 2) map internal layers from the surface to bed with fine vertical resolution better than 1.5 m;
- 3) determine basal conditions and how ice crystal orientation impact ice flow.

In this article, we describe the design and development of the three radar systems together with the associated data processing. We also provide field data collected by these systems in the Summer 2019 deployment at the EGRIP site.

Manuscript received December 2, 2019; revised March 12, 2020; accepted April 20, 2020. Date of publication May 4, 2020; date of current version May 22, 2020. This work was supported in part by the Villum Investigator Project IceFlow under Grant 16572, in part by the European Union's Horizon 2020 Research and Innovation Programme through the Beyond EPICA Oldest Ice (BE-OI) Project under Grant 730258 (BE-OI CSA), in part by the Swiss State Secretariat for Education, Research and Innovation (SERI) under Contract 16.0144, and in part by the University of Alabama for the development of the Remote Sensing Center. (Corresponding author: Jie-Bang Yan.)

Jie-Bang Yan, Linfeng Li, Joshua A. Nunn, Charles O'Neill, Ryan A. Taylor, Christopher D. Simpson, Shashank Wattal, and Prasad Gogineni are with the Remote Sensing Center, University of Alabama, Tuscaloosa, AL 35487 USA (e-mail: jbyan@ua.edu; lli74@crimson.ua.edu; janunn@crimson.ua.edu; croneill@eng.ua.edu; rtaylor@eng.ua.edu; cdsimpson1@crimson.ua.edu; swattal@crimson.ua.edu; sgogineni@ua.edu).

Dorte Dahl-Jensen is with the Centre for Ice and Climate, University of Copenhagen, 1165 Copenhagen, Denmark, and also with the Centre for Earth Observation Science, University of Manitoba, Winnipeg, MB R3T 2N2, Canada (e-mail: ddj@nbi.ku.dk).

Daniel Steinhage and Heinrich Miller are with the Alfred Wegener Institute, Helmholtz Centre of Polar and Marine Research, 27570 Bremerhaven, Germany (e-mail: Daniel.Steinhage@awi.de; Heinrich.Miller@awi.de).

Olaf Eisen is with the Alfred Wegener Institute, Helmholtz Centre of Polar and Marine Research, 27570 Bremerhaven, Germany, and also with the University of Bremen, 28359 Bremen, Germany (e-mail: Olaf.Eisen@awi.de).

Digital Object Identifier 10.1109/JSTARS.2020.2991682

TABLE I
 RADAR SYSTEMS PARAMETERS AND LINK BUDGET

	VHF Radar	UHF Radar	UWB Radar	Unit
Polarization	Linear	Linear	Dual	--
Frequency	200	650/750	260	MHz
Bandwidth	60	100/300	160	MHz
Pulse length	10	10	10	μ s
PRF	5	10	5	kHz
TX power (peak)	4.8	4.8	1.8	kW
AC power consumption (RF electronics only)	0.95	1.5	0.62	kW
Antenna gain (2-way)	25	60	36	dBi
Air-ice trans. coeff.	-0.7	-0.7	-0.7	dB
Ice loss (3 km; 2-way)	60	90	60	dB
Ice bed refl. coeff.	-20	-20	-20	dB
Pulse compression gain	24.8	27/31.8	29	dB
Integration gain (HW)	24	15.1	21.1	dB
Spreading loss term	92.6	92.6	92.6	dB
System losses	3	5	3	dB
Noise figure	3.5	5	3.5	dB
Processing gain	15	15	15	dB
Ice bed SNR	74.2	62	60	dB

Bold values in the table is the key of the figure.

II. RADAR SYSTEM DESIGN

The surface-based radar systems are based on chirped pulse architecture with multiple transmit (TX) and receive (RX) channels. All the three systems share the same digital subsystem, which includes an 8-channel 14-b 2 GSPS arbitrary waveform generator (AWG) and 14-b 1 GSPS digitizer, a GPS recorder, and a computer server to store the recorded data. The AWG allows the amplitude and phase of the radar waveform from each channel to be individually controlled for array calibration. The digitizer has two independent data streams—quick-look and storage. In the quick-look stream, the signal can be coherently averaged up 1000 pulses and then, pulse-compressed to obtain a radar A-scope for real-time display. In the storage stream, up to 256 pulses can be coherently integrated and digitally down converted for real-time storage. The following provides details on the RF electronics design of each system.

A. VHF System

The VHF radar system has four TX and four RX channels. The system parameters are summarized in Table I. The AWG directly synthesizes a chirp from 170 to 230 MHz. For each TX channel, the chirp signal is amplified in two stages to 1.2 kW before feeding to the TX antenna (which is upgraded from the 2018 version reported in [9] in which the peak TX power for each channel is 150 W). The receiver consists of a cascade of a 100-W high-power blanking switch, a bandpass filter (BPF), a limiter, an isolation switch, two low-noise amplifiers (LNA), low-pass filter (LPF), and BPF. Fig. 1 shows the system block diagram. The receiver has an overall gain of 45.7 dB and a noise figure of 2.9 dB. Table I shows a summary of the VHF radar system parameters as well as the estimated link budget.

To characterize the radar impulse response and its loop sensitivity, we performed a loopback test using a single VHF radar

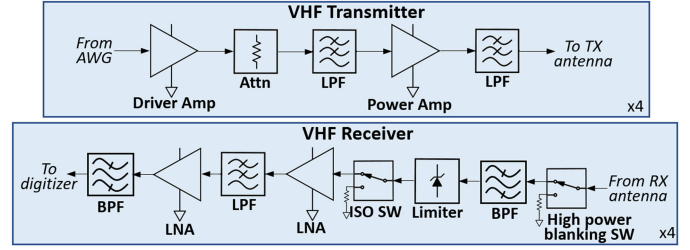


Fig. 1. VHF radar transmitter and receiver block diagram.

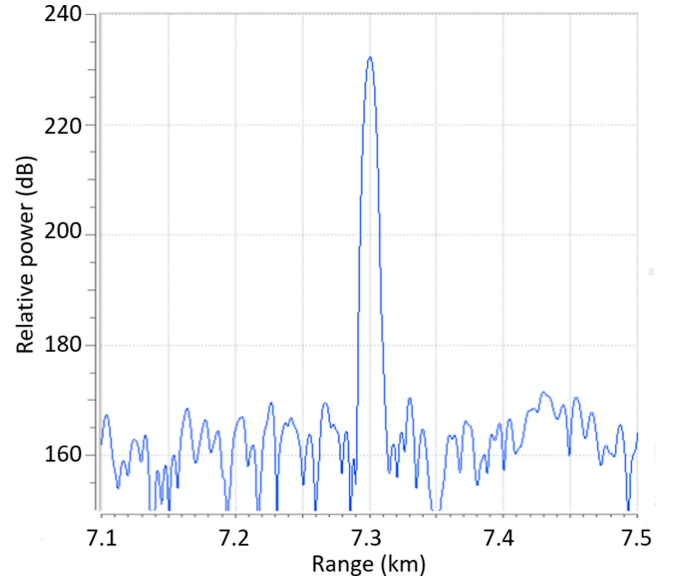


Fig. 2. Measured VHF radar impulse response using a distant point target simulated by an optical delay line and attenuators.

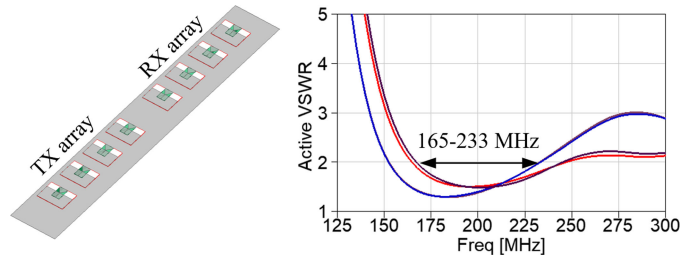


Fig. 3. VHF antenna array (left: array design; right: simulated active VSWR of the TX array).

channel using a 7.3-km long fiber optical delay line and an attenuator chain of 110 dB loss. Fig. 2 shows the measured impulse response after pulse compression and coherent integration in hardware upon receiving. With the measured SNR of 73 dB and the two-way antenna array gain, we estimate that the overall sensitivity would be about 214 dB. With further coherent and incoherent along-track processing of 40 dB or more, a total loop sensitivity of more than 254 dB can be achieved.

A bowtie monopole antenna array is designed for use with the VHF system. The array configuration is different from the 2018 version [9] in that we use separate TX and RX antenna arrays. Fig. 3 shows the antenna array configuration and the

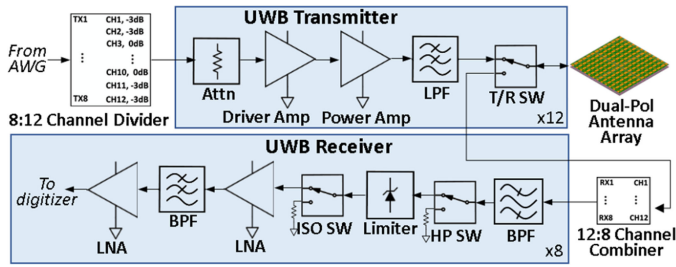


Fig. 4. UWB system block diagram.

active VSWR of the TX array. The antenna array has an overall size of 1.4×8 m with a ground plane spacing of 0.3 m. The center-to-center spacing between the array elements is 0.91 m. Simulation results show that the antenna array has a 2:1 VSWR bandwidth of 68 MHz, from 165 to 233 MHz. The simulated one-way array gain is 12.5 dBi. The closest TX and RX element separation is 1.47 m and the corresponding measured coupling is -25 dB. This makes the 100-W high-power switch in the receiver sufficient to provide the necessary TX-RX isolation.

B. UWB System

For UWB system, the AWG directly synthesizes a chirp with a pulsewidth of $10 \mu\text{s}$ at a duty cycle of 5%. The UWB radar expands the 8-channel digital system outputs to 12 TX channels with power level tapering for feeding a 12×12 elements antenna array. This is done by an active 8:12 channel divider built in the TX chassis. Each of the 12 outputs from channel divider is amplified and filtered through an attenuator, a driver amplifier, a power amplifier, and an LPF. A high-power 100 W T/R switch is then added to switch between T/R modes. The RF signals being fed to the antenna array have tapered power levels: 150 W for eight middle channels, 75 W for four edge channels. This amplitude tapering is to reduce the antenna array edge effect [10]. After the $10\text{-}\mu\text{s}$ transmit window, the T/R switch is set to the receiving mode. The reflected signals from ice internal layers and ice bed are received from the same antenna array and combined back to eight channels, through a passive 12:8 channel combiner before going into the RF receivers. Each receiver channel consists of a cascade of a BPF, a high-power switch, a limiter, an isolation switch, an LNA, a BPF, and another LNA. Fig. 4 shows the high-level block diagram of the UWB radar. By changing the feeding ports at the dual-polarized antenna array, the UWB radar can be operated in both VV and HH polarization. The UWB radar system parameters and link budget are shown in Table I. The measured radar impulse response is shown in Fig. 5. The range sidelobes are 60 dB or lower 30 m away from the peak return. This shows that we can map internal layers with return loss of 80 dB when bed return loss is about 20 dB. The multiple curves represent signal received from the eight receivers. The UWB radar has a loop sensitivity of about 200 dB, excluding additional processing gain resulting from coherent and incoherent gains from along track array processing and speckle reduction.

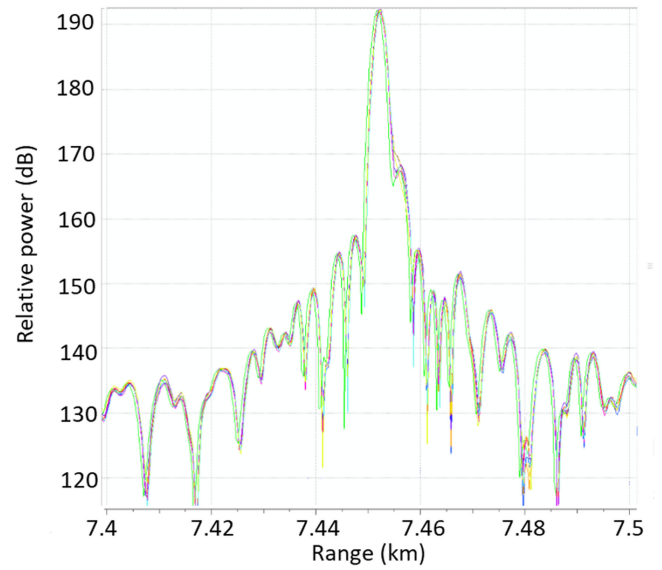


Fig. 5. Measured UWB radar impulse response using a distant point target simulated by an optical delay line and attenuators.

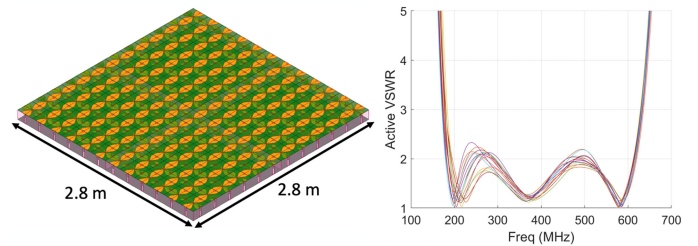


Fig. 6. UWB dual-pol antenna array (left: array design; right: simulated active VSWR).

The dual-polarized antenna array for the UWB radar system is a closely coupled bowtie array which covers the frequency over 180–620 MHz. The whole array is 2.8×2.8 m, which consists of 12×12 dual-polarized antenna elements and a total of 288 ports. The antenna ports in the along-track are precombined at the antenna so that the array has 12 HH ports and 12 VV ports spanned over the cross track. The performance of the antenna array is shown in Fig. 6.

C. UHF System

The 2019 UHF radar has two major changes from the 2018 version reported in [11]: 1) increased peak transmit power from 100 W per channel to 600 W per channel and 2) rearranged antenna array configuration. The UHF radar system parameters are summarized in Table I. Instead of the large 16×17 m cross which is susceptible to array phase center displacement due to rough ice surface, the antenna array has been reconfigured in a T-shape as shown in Fig. 7. Since the number of antenna panels is the same, the overall gain remains the same as the 2018 version.

As the power amplifier of the system was upgraded, we have recharacterized the system impulse response and the result is shown in Fig. 8. With the new amplifier, the overall loop sensitivity of the radar is about 268 dB.

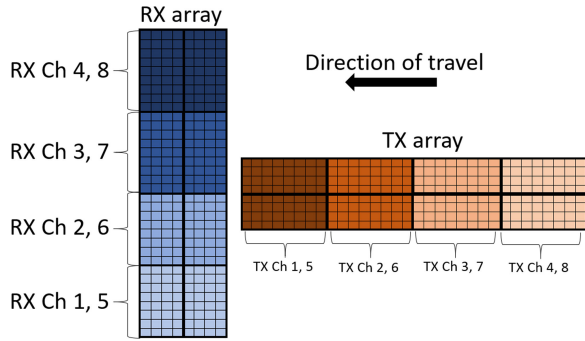


Fig. 7. Rearranged UHF radar antenna array. A small grid represents an antenna element.

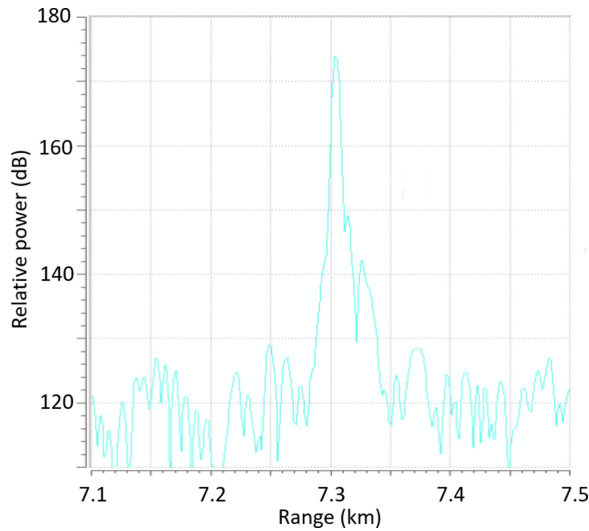


Fig. 8. Measured UHF radar impulse response using a distant point target simulated by an optical delay line and attenuators.

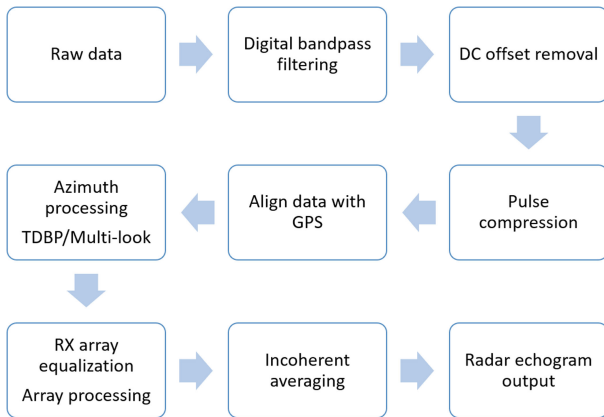


Fig. 9. Signal processing flowchart.

III. DATA PROCESSING

Raw radar data are ingested into MATLAB for radar echogram generation. The process flow is summarized in Fig. 9. It follows a standard radar data processing procedure in which data are first digitally bandpass filtered to remove out-of-band noise and then, undergo a dc offset removal. The data are then pulse-compressed

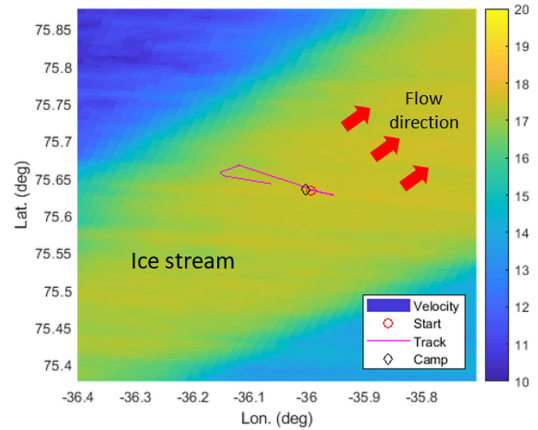


Fig. 10. Survey track for the example VHF radar data in Fig. 10 collected near EGRIP site. The background is the velocity field of the ice stream [14].

in the range domain and aligned with GPS data. After that, the data are SAR processed in the azimuth direction with two algorithm options: 1) conventional time-domain back projection (TDBP) [12] or 2) TDBP with along-track multilook (ML) [13]. The second method adds phase shifts to samples over the along-track aperture to synthesize an along-track beam steered towards an off-nadir angle. As an example, VHF radar data collected along the track shown in Fig. 10 are processed with the above two methods and the results are compared in Fig. 11. The vertical line near at the along-track distance of 1.8 km is due to the sharp turnaround of the tracked vehicle. The region between 8 and 10 km shows different internal structure because the tracked vehicle turned into the direction parallel to the ice flow. The ML radar echogram was generated by incoherently combining looks from along-track angles -5° , 0° (nadir), and $+5^\circ$. The advantage of the ML method is that it not only reduces speckle noise, but also recovers the internal layers with positive and negative slope in the along-track direction as indicated by the red arrows in the figure. The layers pointed by the green arrow are not recovered through along-track ML and the implication will be discussed shortly after.

After the along-track processing, echograms generated from each radar receive channel are amplitude and phase equalized and then combined coherently to improve SNR. Fig. 12 shows an example of array processing gain as a result of combining four VHF receive channels. Comparing Fig. 12(a) and (b), the deep layers at 2–2.4 km depth are apparently stronger after the array combining. The bottom internal layers also become stronger after array combining and the signal of the ice bed is improved by about 10.5 dB as evident from radar A-scope comparison shown in Fig. 12(c). As a reference, the theoretical signal voltage gain by combining N channels is $20\log_{10}(N)$ [15]. The minor discrepancy between achieved and ideal gain can be attributed to the roughness of the ice bed interface. The resulting SNR of the ice bed, after array combining, is about 64 dB, which is about 10 dB lower than the estimated SNR in the link budget given in Table I. Such a discrepancy can be attributed to underestimated ice loss as well as planar ice bed assumption.

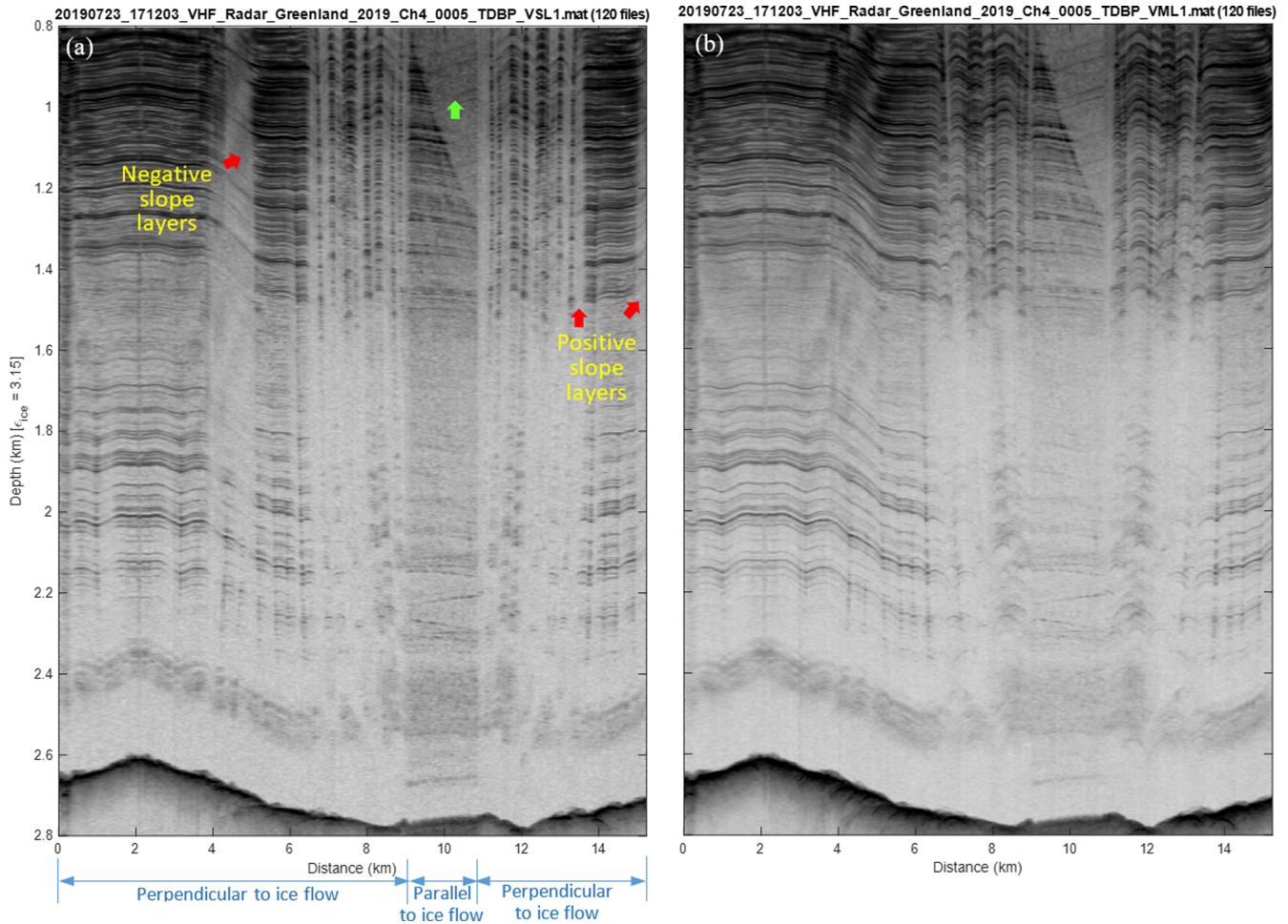


Fig. 11. Comparison between radar echograms generated using (a) conventional TDBP and (b) TDBP with along-track multilook.

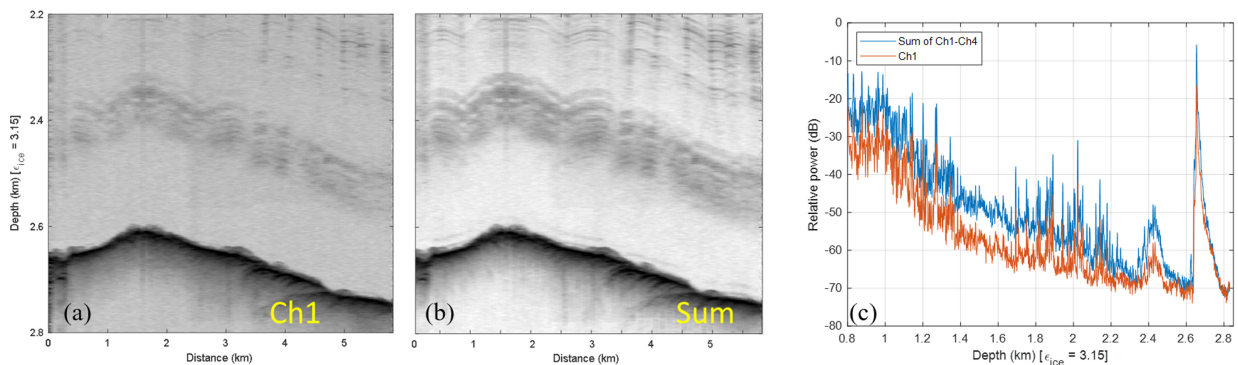


Fig. 12. (a) Zoom-in of the single-channel radar echogram in Fig. 10(a). (b) Radar echogram after array combining. (c) Comparison between radar A-scopes from (a) and (b).

Advanced array combining methods such as minimum variance distortionless response (MVDR) can be used to suppress clutter from airborne ice sounding data as discussed in [16]. Here, for the study of ice sheet's internal structure using surface-based radars, we can synthesize echograms that correspond to different cross-track angles by applying the appropriate phase shifts to each of the channel data. This is a similar concept as the along-track ML processing but in the orthogonal direction. Fig. 13 shows the single-look VHF radar echograms that

correspond to receive beam pointing at cross-track angles -30° , 0° (nadir), and $+30^\circ$. As expected, the nadir echogram has the highest SNR for the bottom layers and bed because the nadir beam captures the most backscattered energy. It is interesting to see that the top layers of the -30° echogram are quite different from those in the other two echograms. To bring out the differences between the echograms, they are combined using RGB coding and the resultant composite echogram is shown in Fig. 13(d). Here, red, green, and blue denote signals from

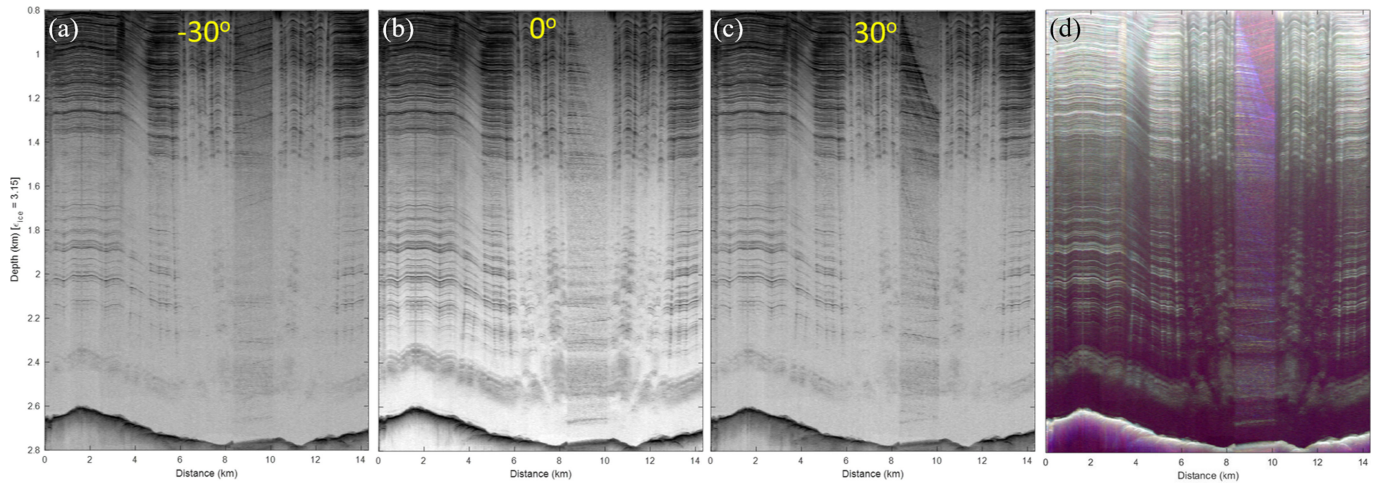


Fig. 13. Radar echograms with receive beam steered to: (a) -30° (left); (b) 0° (nadir); (c) $+30^\circ$ (right); (d) three echograms combined in RGB color where red, green, and blue denote signals from -30° , 0° , and $+30^\circ$, respectively.

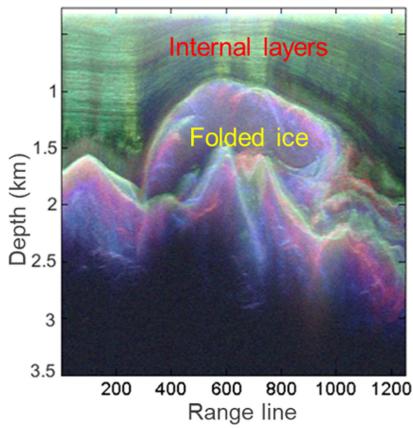


Fig. 14. Composite RGB echogram processed using the data collected from CRISIS multichannel coherent radar depth sounder [16].

-30° , 0° , and $+30^\circ$, respectively, and white thus represents the signal received from all the three directions. For top layers ($\sim 0.8\text{--}1.3$ km in depth), the layers mostly appear as white as they reflect sufficient energy to be captured by the three beams. As it goes deeper, the internal layers appear as green. This is because the backscatter signals from these layers have to undergo more loss and are mostly captured by the nadir beam. Since the ice bed has a very high SNR (~ 64 dB), it appears white in the RGB composite echogram. Beyond the ice bed, off-nadir backscatters due to rough interface can be observed as purple which is a mix of blue and red. Between the along-track distances of 8 and 10 km, the layers at the top appear as red, indicating that layers are sloped in the cross track. This also explains why the layers [indicated by the green arrow in Fig. 11(a)] are not recovered from the along-track ML processing [see Fig. 11(b)].

The same method can be applied to airborne multichannel radar data to reveal the 3-D structure of folded ice under the polar ice sheets. As an example, we have processed the radar data collected by CRISIS in 2009 over the Gamburtsev Subglacial Mountains, East Antarctica [17], using the above-mentioned



Fig. 15. Photos of the UHF radar antenna array (left) and the dual-polarized UWB radar antenna array towed behind the tracked vehicle carrying the radar electronics.

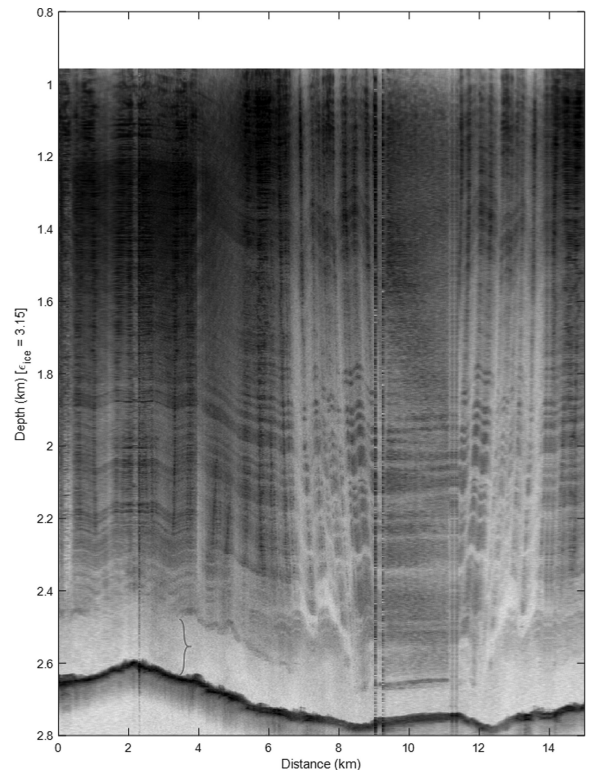


Fig. 16. UHF radar echogram (600–700 MHz).

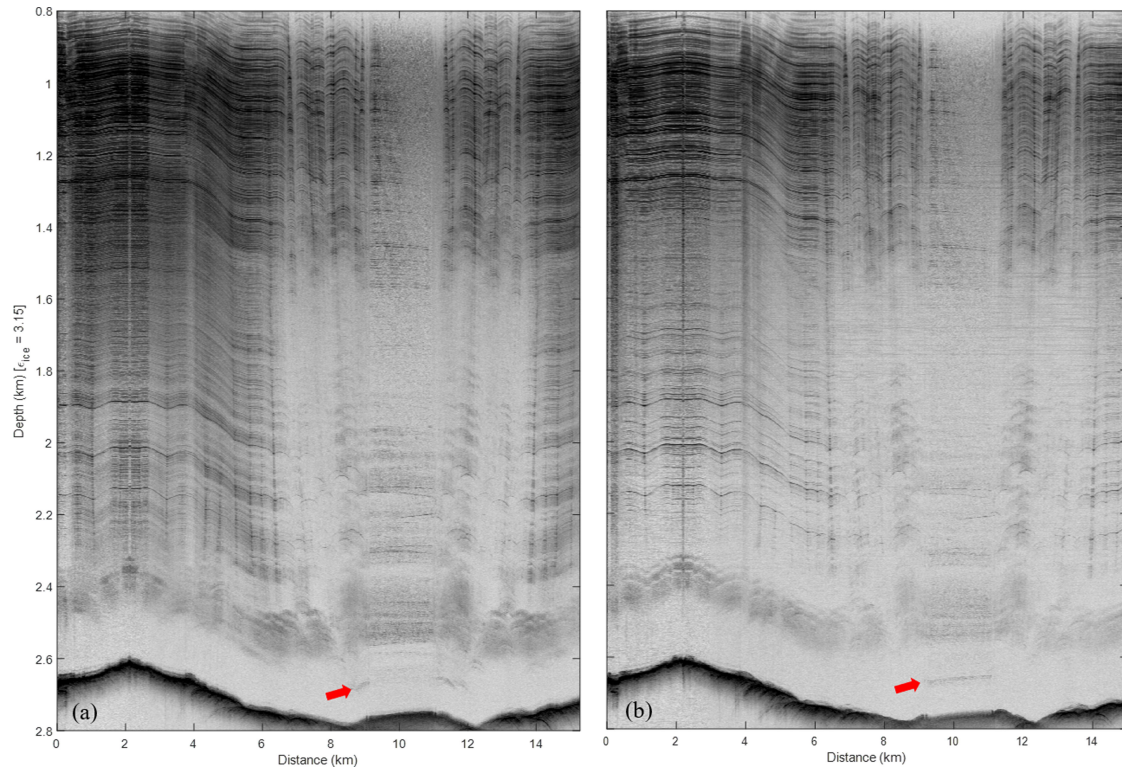


Fig. 17. UWB radar echograms: (a) VV-polarization and (b) HH-polarization.

method. The resultant RGB composite echogram is shown in Fig. 14. It clearly showed that the folded structure underneath the ice sheet is a 3-D structure. Further array processing techniques have been demonstrated to perform 3-D tomography of ice bed [18].

IV. FIELD RESULTS AND DISCUSSIONS

We deployed the three surface-based radar systems to EGRIP in Summer 2019 to assist in the study of the ice sheet structure along the Northeast ice stream. Fig. 15 shows photos of the UHF antenna array and the dual-polarized UWB array towed behind the track vehicle. We placed metallic masts on top of the UHF antenna panels to minimize array displacement.

For comparison, we ran the three radar systems over the same survey line as shown in Fig. 10. The corresponding VHF radar echogram can be found in Fig. 11(b), whereas the UHF and the UWB radar echograms are given in Figs. 16 and 17, respectively. Since the three systems have different number of channels and antenna array configurations, for the purpose of comparison, only single-channel echograms are shown here. They are all processed with TDBP algorithm with three look angles at -5° , 0° , and $+5^\circ$. From the analysis in [11], we found that the ice loss over 600–700 MHz is significantly less than that over 800–900 MHz; we present the sub-banded (600–700 MHz) UHF radar result here. The SNR of the bed for all the three systems ranges from 40 dB to above 60 dB, depending on areas with different roughness and dielectric contrast. The VHF radar echogram appears to be very similar to the HH-polarized UWB radar echogram. Fig. 18 shows a detailed comparison between the

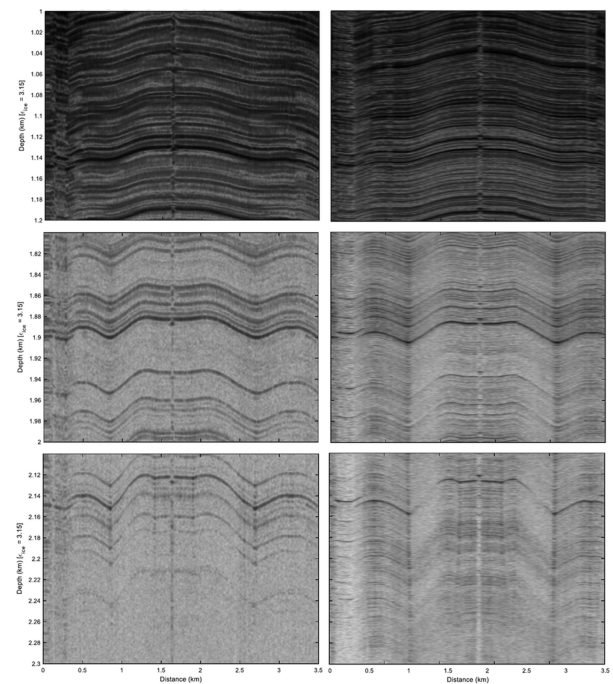


Fig. 18. Comparison between VHF (left panels) and UWB (right panels) radar echograms at different depth ranges (top: 1–1.2 km; middle: 1.8–2 km; bottom: 2.1–2.3 km). The middle vertical feature is caused by sharp turnaround of the tracked vehicle.

VHF and the HH-polarized UWB radar echograms at different depths. The UWB radar echogram shows much finer details on the internal layers than the VHF counterpart as it has 2.7 times

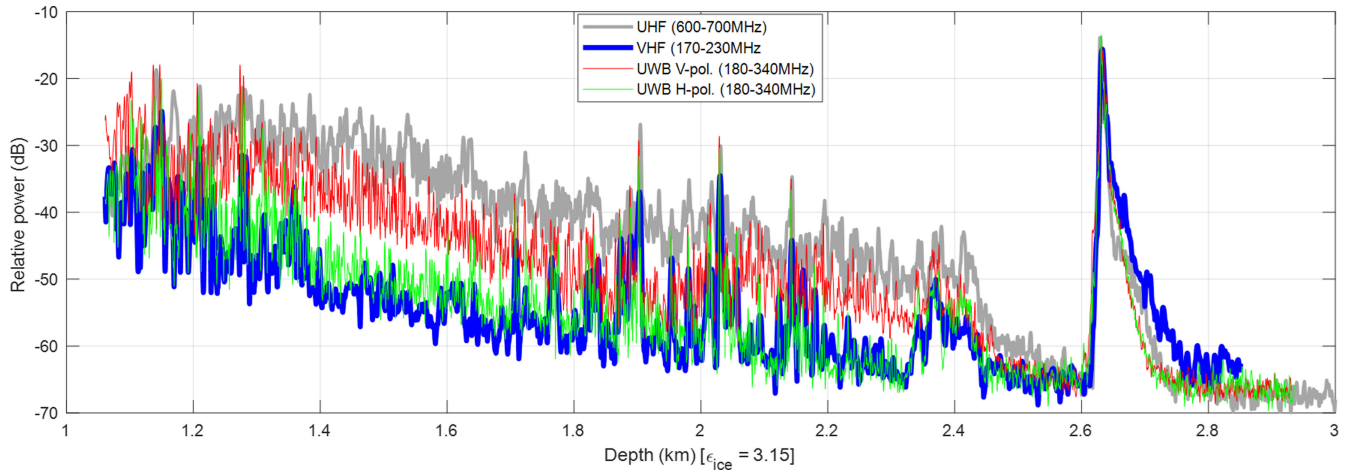


Fig. 19. Comparison between A-scopes obtained from different radar systems obtained at along-track distance of 2 km from the start of the echogram.

higher vertical resolution (0.94 versus 2.5 m). Comparing UWB radar echograms shown in Fig. 17, it is interesting to find that internal layers have a stronger backscatter for VV-polarization than for HH-polarization when the direction of survey is perpendicular to the ice flow (especially between along-track distance 0–4 km). When the direction of survey is parallel to the ice flow, the HH-polarized echogram shows a layer at a depth of about 2.65 km, which cannot be seen in the VV-polarized echogram (as indicated by the red arrows in the figure). Such a difference is likely to be caused by the change of ice crystal orientation at the bottom of the ice along the ice stream. These results demonstrate that a dual-polarized radar can provide additional information on the fabric of ice and how it is related to ice dynamics.

Fig. 19 shows the radar A-scopes obtained from the data shown in Figs. 11(b), 16, and 17 at an along-track distance of 2 km for further comparison. All the three radars can capture the three major englacial events at depths of 1.90, 2.03, and 2.14 km. As we have seen previously, the VHF data are very similar to the UWB H-pol. data in terms of SNR roll off, except that the UWB data show a finer variation (finer internal layers). The UWB V-pol. data have about 10 dB higher backscatter for the internal layers than the V-pol. data. The UHF data have even higher backscatter than the UWB V-pol. data, implying that UHF frequencies are more sensitive to dielectric changes than VHF frequencies. At a depth of about 2.5 km, the UHF radar measures higher backscattered signals than the other low-frequency radar systems and the signals are about 7 dB above the noise floor. We can indeed identify these backscattered signals in the radar echogram shown in Fig. 16, in which these signals, as indicated by the curly bracket, appear as volume scattered signals. The presence of these volume scattered signals at the boundary layer may indicate that there is a mixing of ice underneath the moving ice sheet and these signals can only be captured by radars operating at high frequencies.

V. CONCLUSION

We have designed and developed three surface-based multi-channel radar systems operating over different frequency bands

and polarizations for the measurements of polar ice sheets. Field results obtained from the 2019 EGRIP deployment are presented in this article. From these results, we have shown how the multiphase center data can be processed with along-track ML and array processing to reveal how the internal layers change in the along-track and cross-track directions. Results from the dual-polarized UWB radar have demonstrated that more internal layers can be imaged with the additional bandwidth as compared to the “narrowband” VHF radar, and that the selection of measurement polarization is important even for nadir sounding systems as it can help reveal different internal layers in the ice sheets. As compared to systems operating at VHF, UHF radar results have shown enhanced sensitivity to dielectric changes and volume scattering signals bands, which may be of interest to the study of ice-bed boundary condition and boundary layer mixing. This demonstrates that radars operating at frequencies as high as 850 MHz provide opportunities for further research to develop airborne and spaceborne radars for complete mapping of large ice sheets in Antarctica and Greenland.

ACKNOWLEDGMENT

The authors would like to thank the Senior Electronic Technician S. Jones and Engineer D. Elluru, and the undergraduate research assistant team at the University of Alabama for helping with the construction of the radar systems and antenna arrays. The authors would also like to thank Dr. S. Gurbuz, Dr. Z. Jiang, and Dr. D. Tao and their students for their help with radar data format conversion and storage. The authors would also like to thank the EGRIP logistic support and field personnel, and the U.S. Air National Guard flights provided by the U.S. National Science Foundation.

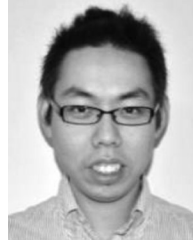
EGRIP is directed and organized by the Center of Ice and Climate at the Niels Bohr Institute. It is supported by funding agencies and institutions in Denmark (A. P. Møller Foundation, University of Copenhagen), USA (U.S. National Science Foundation, Office of Polar Programs), Germany (Alfred Wegener Institute), Japan (National Institute of Polar Research and Arctic

Challenge for Sustainability), Norway (University of Bergen and Bergen Research Foundation), Switzerland (Swiss National Science Foundation), France (French Polar Institute Paul-Emile Victor, the Institute for Geosciences and Environmental research), and China (Chinese Academy of Sciences and Beijing Normal University).

The Beyond EPICA-Oldest Ice (BE-OI) Project is also supported by national partners and funding agencies in Belgium, Denmark, France, Germany, Italy, Norway, Sweden, Switzerland, The Netherlands, and the United Kingdom. The opinions expressed and arguments employed herein do not necessarily reflect the official views of the European Union funding agency, the Swiss Government, or other national funding bodies. This is BE-OI publication number 9.

REFERENCES

- [1] R. Alley, M. Spencer, and S. Anandakrishnan, "Ice-sheet mass balance: Assessment, attribution and prognosis," *Ann. Glaciology*, vol. 46, pp. 1–7, 2007.
- [2] Arctic Monitoring and Assessment Programme, "Summary – The Greenland Ice Sheet in a changing climate: Snow, water, ice and permafrost in the Arctic (SWIPA)," 2009. [Online]. Available: <https://www.amap.no/documents/doc/the-greenland-ice-sheet-in-a-changing-climate-snow-water-ice-and-permafrost-in-the-arctic-full-version/714>
- [3] E. Rignot, I. Velicogna, M. van den Broeke, A. Monaghan, and J. Lenaerts, "Acceleration of the contribution of the Greenland and Antarctic ice sheets to sea level rise" *Geophys. Res. Lett.*, vol. 38, no. 5, 2011, Art. no. L05503.
- [4] D. Vaughan and R. Arthern, "Why is it hard to predict the future of ice sheets?," *Science*, vol. 315, no. 5818, pp. 1503–1504, 2007.
- [5] J. Johnson and J. Fastook, "Northern Hemisphere glaciation and its sensitivity to basal melt water," *Quaternary Int.*, vol. 95, pp. 65–74, 2002.
- [6] T. Kyrke-Smith, R. Katz, and C. Fowler, "Subglacial hydrology and the formation of ice streams," *Proc. Roy. Soc. A*, vol. 470, no. 2161, 2014, Art. no. 20130494.
- [7] T. Kleiner and A. Humbert, "Numerical simulations of major ice streams in western Dronning Maud Land, Antarctica, under wet and dry basal conditions," *J. Glaciology*, vol. 60, no. 220, pp. 215–232, 2014.
- [8] East Greenland ice-core project, 2018. [Online]. Available: <https://eastgrip.org/>
- [9] J.-B. Yan *et al.*, "Surface-based multi-channel radar systems for ice sheet measurements," in *Proc. IEEE Int. Symp. Geosci. Remote Sens.*, 2019, pp. 1001–1004.
- [10] L. H. Yorinks, "Edge effects in low-sidelobe phased array antennas," in *Proc. IEEE Antennas Propag. Soc. Int. Symp.*, Vancouver, Canada, Jun. 1985, pp. 225–228.
- [11] J.-B. Yan *et al.*, "UHF radar sounding of polar ice sheets," *IEEE Geosci. Remote Sens. Lett.*, to be published, doi: [10.1109/LGRS.2019.2942582](https://doi.org/10.1109/LGRS.2019.2942582).
- [12] A. F. Yegulalp, "Fast backprojection algorithm for synthetic aperture radar," in *Proc. IEEE Radar Conf. Radar Next Millennium*, Waltham, MA, USA, 1999, pp. 60–65.
- [13] A. Mishra, J.-B. Yan, C. J. Leuschen, and S. Gogineni, "Multilook SAR processing and array optimization applied to radio echo ice sounding data," in *Proc. IEEE Int. Symp. Phased Array Syst. Technol.*, Waltham, MA, USA, 2016, pp. 1–5.
- [14] I. Joughin, B. Smith, I. Howat, T. Scambos, and T. Moon, "Greenland flow variability from ice-sheet-wide velocity mapping," *J. Glaciology*, vol. 56, pp. 415–430, 2010.
- [15] H. Van Trees, *Optimum Array Processing*. New York, NY, USA: Wiley-Interscience, 2002.
- [16] J. Li *et al.*, "High-altitude radar measurements of ice thickness over the Antarctic and Greenland ice sheets as a part of Operation IceBridge," *IEEE Trans. Geosci. Remote Sens.*, vol. 51, no. 2, pp. 742–754, Feb. 2013.
- [17] "CRISIS: Radar depth sounder data," Univ. Kansas, Lawrence, KS, USA, 2009. [Online]. Available: <http://data.cresis.ku.edu/>
- [18] J. Paden, T. Akins, D. Dunson, C. Allen, and P. Gogineni, "Ice-sheet bed 3-D tomography," *J. Glaciology*, vol. 65, no. 195, pp. 3–11, 2010.



Jie-Bang Yan (Member, IEEE) received the B.Eng. (first class honors) degree in electronic and communications engineering from the University of Hong Kong, Hong Kong, in 2006, the M.Phil. degree in electronic and computer engineering from the Hong Kong University of Science and Technology, Hong Kong, in 2008, and the Ph.D. degree in electrical and computer engineering from the University of Illinois at Urbana–Champaign, Champaign, IL, USA, in 2011.

From 2009 to 2011, he was a Croucher Scholar with the University of Illinois at Urbana–Champaign, where he was involved in MIMO and reconfigurable antennas. In 2011, he joined the Center for Remote Sensing of Ice Sheets, University of Kansas, Lawrence, KS, USA, as an Assistant Research Professor. He is currently an Assistant Professor of Electrical and Computer Engineering and the Founding Deputy Director of the Remote Sensing Center, University of Alabama, Tuscaloosa, AL, USA. He also has extensive airborne and ground-based radar deployment experience in both domestic and international regions, including Greenland and Antarctica. He holds two U.S. patents and two U.S. patent applications related to novel antenna technologies. His current research interests include the design and analysis of antennas and phased arrays, ultrawideband radar systems, radar signal processing, and remote sensing.

Dr. Yan was the recipient of multiple research awards, including the Best Paper Award, in the 2007 IEEE (HK) AP/MTT Postgraduate Conference, the UIUC Raj Mittra Outstanding Research Award, in 2011, the NASA Group Achievement Award, in 2013, the Best Paper Finalist of the 2015 National Instruments Week, and the UA CoE Research and Innovation Award, in 2019. He is a Technical Reviewer for several journals and conferences on antennas and remote sensing.



Linfeng Li was born in Kunming, China, in 1992. He received the B.S. degree in electrical engineering from the Beijing University of Chemical Technology, Beijing, China, in 2015. He is currently working toward the Ph.D. degree in electrical engineering from the University of Alabama (UA), Tuscaloosa, AL, USA.

In 2017, he joined the Remote Sensing Center (RSC), UA, as a Graduate Research Assistant. Since then, he has been involved in the development of multiple radar systems for polar ice sounding. His current research interest includes antenna and phased array design, RF/microwave component design, and ultrawideband radar system design.



Joshua A. Nunn received the master's degree in electrical engineering from the University of Alabama, Tuscaloosa, AL, USA, in December 2019.

While completing the degree, he was a Research Assistant with Alabama's Remote Sensing Center and specialized in radar system and RF circuit design. He is currently working with Redstone Arsenal, Huntsville, AL, USA.



Dorte Dahl-Jensen received the M.Sc. and Ph.D. degrees in geophysics from the University of Copenhagen, Copenhagen, Denmark, in 1984, and 1988, respectively.

She is currently a Professor with the Niels Bohr Institute, University of Copenhagen, and the Canada Excellence Research Chair with the Centre for Earth Observation Science, University of Manitoba, Winnipeg, MB, Canada. Her major scientific achievements have been in leading ice core drilling and subsequent analysis of ice core data in conjunction with models to determine past climate and how it affected the Greenland ice sheet. She has led several international deep drilling projects such as NGRIP, NEEM, and EGRIP. In addition, she has led large research projects funded by grants from the Danish National Research Foundation (DNRF), European Research Council (ERC), EU FP7, Villum Investigator, and Canada Excellence Research Chair. The research has led to numerous achievements and here are some highlights to illustrate how the past illuminates potential future abrupt climate changes. During the Last Interglacial where Greenland temperatures were 5 °C warmer than the present, the Greenland ice sheet thinned and contributed to the global sea level rise by about 2 m. Dated Greenland ice cores through the past 2000 years show the impact on the atmosphere from human activities, such as forest burning and industrialization, and from volcanic eruptions producing aerosols that cool the earth surface for about ten summers following the event. Synchronized ice cores from Greenland and Antarctica show 25 very abrupt climate changes during the last glacial and modeling shows that the events represent internal movement of energy through ocean and atmosphere between the Northern and Southern hemispheres. The research is very well cited, and five others and Prof. Dahl-Jensen from her research group are Thomson Reuters highly cited researchers.



Charles O'Neill received the B.S. degree in aerospace engineering, the M.S. degree in mechanical engineering, and the Ph.D. degree in aerospace engineering from Oklahoma State University, Stillwater, OK, USA, in 2001, 2003, and 2011 respectively.

He was with Textron/Cessna Aircraft for prototype aircraft development, with the University of Alabama, Tuscaloosa, AL, USA, as an Assistant Professor, and with the Remote Sensing Center for aerial and surface-based remote sensing. He holds manned and unmanned FAA pilot licenses.



Ryan A. Taylor received the B.S. and M.S. degrees in electrical engineering from the University of Alabama, Tuscaloosa, AL, USA, in 2008 and 2011, respectively, and the Ph.D. degree in electrical and computer engineering from Mississippi State University, Mississippi State, MS, USA, in 2018.

He is an Assistant Professor of electrical and computer engineering with the Remote Sensing Center, University of Alabama. His research interests include digital and embedded systems and remote sensing of the earth.



Christopher D. Simpson received the B.S. degree in aeronautics and astronautics engineering from Purdue University, West Lafayette, IN, USA, in 2010, the M.S. degree in aerospace engineering and mechanics, in 2016 from The University of Alabama (UA), Tuscaloosa, AL, USA, where he is currently working toward the Ph.D. degree in aerospace engineering in mechanics.

He is a Graduate Research Assistant with the Remote Sensing Center, UA.



Shashank Wattal received the bachelor's degree in computer engineering, working on electrical sensors and device simulation, from the University of Alabama (UA), Tuscaloosa, AL, USA, in 2017, where he is currently working toward the graduate degree with the Remote Sensing Center, working on signal processing algorithms for FMCW and pulsed radar arrays for cryosphere remote sensing.

He is also a Research Assistant with the Remote Sensing Center, UA.



Daniel Steinhage received the Diploma from the Westfälische Wilhelms University Münster, Münster, Germany, in 1994, and the Ph.D. degree from University of Bremen, Bremen, Germany, in 2000, both in geophysics.

He is a Senior Scientist with the Alfred Wegener Institute, Helmholtz Center for Polar and Marine Research, Bremerhaven, Germany, participating in and leading several expeditions in polar regions, performing airborne, and ground-based radar surveys. He is currently the Coordinator of AWT's research aircraft.



Prasad Gogineni (Life Fellow, IEEE) received the Ph.D. degree in electrical engineering from the University of Kansas (KU), Lawrence, KS, USA, in 1984.

He is currently the Cudworth Professor with the Department of Electrical and Computer Engineering and the Department of Aerospace Engineering and Mechanics, and the Founding Director of the University of Alabama, Tuscaloosa, AL, USA. He was formerly a Deane E. Ackers Distinguished Professor with KU, where he was the Director of the National Science Foundation Science and Technology with the

Center for Remote Sensing of Ice Sheets. He developed several radar systems that are currently being used at KU for the sounding and imaging of polar ice sheets. He has also participated in field experiments in the Arctic and Antarctica. He has authored or co-authored more than 90 archival journal publications, 200 technical reports, and conference presentations. His current research interests include the application of radars to the remote sensing of the polar ice sheets, sea ice, ocean, atmosphere, and land.

Dr. Gogineni is a Member of the International Union of Radio Science, the American Geophysical Union, the International Glaciological Society, and the Remote Sensing and Photogrammetry Society. He was an Editor for the *IEEE Geoscience and Remote Sensing Society Newsletter* from 1994 to 1997.



Heinrich Miller received the diploma and Ph.D. degrees in geophysics from the University of Munich, Munich, Germany, in 1969 and 1971, respectively, where he did research in deep structures of orogenesis as well as glaciology.

From 1985 to 2012, he was a Professor of Geophysics with the University of Bremen, Bremen, Germany, and led research groups in geophysics and glaciology at the Alfred-Wegener Institute, Helmholtz Center for Polar and Marine Research, Bremerhaven, Germany. Here, he was a Deputy Director from 2000 to 2012 and since then, he has been Emeritus Professor with the University of Bremen and holds a Helmholtz Professorship in Glaciology. He has participated and led many research expeditions both in marine geophysics as well as for glaciological field work in particular in the application of geophysical techniques to glaciological problems.



Olaf Eisen received the diploma from the Technical University of Karlsruhe, Karlsruhe, Germany, where he performed research on the contribution of sea ice to the ocean–ice–atmosphere interaction, and the Ph.D. degree working on the nature of electromagnetic reflection in ice from the University of Bremen (UB), Bremen, Germany, in 2003.

Since 1999, he has been with the Alfred-Wegener Institute (AWI), Helmholtz Center for Polar and Marine Research, Bremerhaven, Bremerhaven, Germany. During stays at the University of Alaska, Fairbanks, AK, USA, (2000) and the ETH Zürich, Zürich, Switzerland (2005–2006), he conducted research on the interaction of climate and ice dynamics. From 2008 to 2013, he led an Emmy Noether Young Investigators Group, University of Heidelberg, Heidelberg, Germany, and AWI, applying geophysical methods on ice sheets and glaciers, with habilitation, in 2010 and Associated Professorship, in 2013. Since 2014, he has been a Joint Professor for Glaciology with AWI, focusing on the application of geophysical methods in cryospheric research.